The Journal of Antibiotics (2017) 70, 90–95

www.nature.com/ja

ORIGINAL ARTICLE

Xantholipin B produced by the *stnR* inactivation mutant *Streptomyces flocculus* CGMCC 4.1223 WJN-1

Sifan Wu[1], Tingting Huang[1], Dan Xie[1], Jing Wo, Xiaozheng Wang, Zixin Deng and Shuangjun Lin

Xantholipin is a polycyclic xanthone antibiotic that exhibits potent cytotoxic and antibacterial activity. In this study, a new xanthone-type antibiotic, xantholipin B (1), was isolated for the first time along with its known derivative, xantholipin (2), from strain WJN-1, an aminotransferase inactivation mutant of the streptonigrin-producer *Streptomyces flocculus* CGMCC 4.1223. The structure of 1 was established based on spectroscopic analysis and supports the previously proposed biosynthetic pathway as a key intermediate of 2. Moreover, 1 showed 3- to 10-fold greater cytotoxicity than 2 against a select panel of human cancer cell lines. In addition, 1 demonstrated powerful antimicrobial activity against both Gram-positive bacteria and fungi. Importantly, both 1 and 2 inhibited the methicillin-resistant strain *Staphylococcus aureus* Mu50, with the MIC value of 0.025 μg ml^{-1}. The new structural features of 1 enrich the structural diversity of xantholipin family compounds and shed new light on the structure–activity relationship of 1 as a promising antitumor drug candidate.
The Journal of Antibiotics (2017) **70,** 90–95; doi:10.1038/ja.2016.60; published online 22 June 2016

INTRODUCTION

Natural products and their mimics have represented a substantial market share in the pharmaceutical industry from the 1980s through the 2010s, comprising ~75% of anticancer compounds and 50% of anti-infectives.[1] Microorganisms, especially the actinobacteria, are renowned as prolific sources of natural products with diverse biological activities. Genome sequence analysis has revealed the presence of ~25 secondary metabolite gene clusters per genome on average, representing the potential for the discovery of new compounds. However, the potential secondary metabolite gene clusters far outnumber the secondary metabolites identified because of silent or cryptic biosynthetic gene clusters under classical laboratory conditions in either the native or heterologous hosts, making the discovery of new metabolites quite challenging.[2–4] To solve these problems, numerous approaches have been developed to activate silent or cryptic biosynthetic gene clusters.[5–8]

Xantholipin (XAN, **2**), a xanthone-derived natural product with a hexacyclic angular fused skeleton, was first isolated from *Streptomyces flavogriseus* in 2003.[9] XAN contains a xanthone core scaffold, a methylene dioxybridge and a *δ*-lactam structure that is commonly present in polycyclic xanthone antibiotics. XAN also features a chlorine atom attached at C-l in the xanthone nucleus. Several similar xanthone antibiotics have been reported, including lysolipin I,[10] albofungine,[11] actinoplanones,[12,13] cervinomycins[14–16] and LL-D42067α.[17] Polycyclic xanthone family members generally exhibit powerful antimicrobial and antitumor activities. XAN itself possesses potent cytotoxicity against the leukemia cell line HL-60 (IC_{50} <0.3 μM) and the oral squamous carcinoma cell line KB (IC_{50} <2 nM).[9] XAN also demonstrates activity against Gram-positive bacteria, including methicillin-resistant *Staphylococcus aureus* and vancomycin-resistant *Enterococcus faecalis*. In addition, XAN inhibits HSP47 gene expression, with an IC_{50} value of 0.20 μM, and demonstrates cytostatic activity, with an IC_{50} of 80 nM.[9]

The 52-kb XAN biosynthetic gene cluster has been identified in *S. flavogriseus* and reveals type II polyketide synthases, regulators and tailoring enzymes responsible for the formation of the unusual functional groups.[18] Type II polyketide synthases form the nascent polyketide intermediate, and the *in vivo* work confirmed that xanthone scaffold formation is catalyzed by the FAD (flavin adenine dinucleotide)-binding monooxygenase XanO4, with tailoring steps including the formation of the σ-lactam moiety by the asparagine synthetase XanA, the methylene dioxy bridge by the *P*450 monooxygenase XanO2 and the hydrolysis of the carbon backbone by the FAD-binding monooxygenase XanO5.[18]

Here, we report the construction of a *stnR* replacement mutant (designated WJN-1) of the streptonigrin producer *Streptomyces flocculus* CGMCC4.1223. Comparative metabolite profiling revealed two compounds apparently unrelated to streptonigrin biosynthesis that accumulated in strain WJN-1. These two compounds were purified, and their structures were elucidated by extensive 1D and 2D NMR spectroscopies (Figure 1). Compound **2** was identified as XAN by comparison with the previously reported NMR and MS data

State Key Laboratory of Microbial Metabolism, Joint International Laboratory on Metabolic & Developmental Sciences, School of Life Sciences & Biotechnology, Shanghai Jiao Tong University, Shanghai, People's Republic of China
[1]These three authors contributed equally to this work.
Correspondence: Professor S Lin, State Key Laboratory of Microbial Metabolism, Joint International Laboratory on Metabolic & Developmental Sciences, School of Life Sciences & Biotechnology, Shanghai Jiao Tong University, 800 Dongchuan Road, Shanghai 200240, People's Republic of China.
E-mail: linsj@sjtu.edu.cn
Received 17 January 2016; revised 20 March 2016; accepted 27 April 2016; published online 22 June 2016

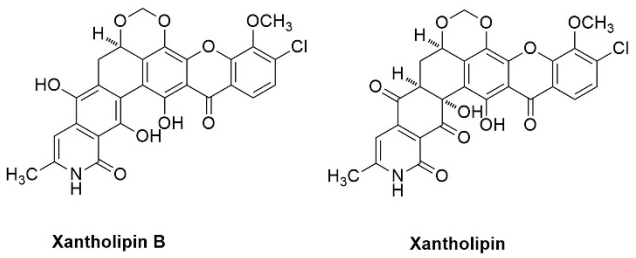

Figure 1 The structures of xantholipin B (**1**) and xantholipin (**2**).

for xantholipin.[9] Compound **1** was designated as a new XAN derivative, named xantholipin B, that could be a biosynthetic precursor of **2**.[18] Moreover, **1** demonstrates significant antitumor and antimicrobial activity. The new compound not only shows better bioactivity but its identification also provides an opportunity to understand the unusual modifications involved in the biosynthesis of other polycyclic xanthone antibiotics.

RESULTS AND DISCUSSION

StnR in the formation of a β-methyltryptophan moiety in the streptonigrin biosynthetic pathway

Streptonigrin is an aminoquinone antitumor antibiotic produced by *S. flocculus* CGMCC4.1223, and its biosynthetic gene cluster was identified by genome scanning.[19] Previous feeding experiments with isotopically labeled precursors suggested that the 4-phenylpicolinic acid moiety of streptonigrin is formed by cleavage of the indole ring originating from L-tryptophan via β-methyltryptophan.[20,21] Biosynthesis of β-methyltryptophan is catalyzed by three proteins: StnR, StnK3 and StnQ1. StnR was identified as a homolog of a pyridoxal 5′-phosphate-dependent aminotransferase, whereas StnK3 and Q1 are designated as a cupin-fold protein and an *S*-adenosylmethionine-dependent C-methyltransferase, respectively. The L-tryptophan is transaminated by the aminotransferase StnR to give indolepyruvate that is converted to β-methylindolepyruvate by StnQ1. Subsequently, StnK3 catalyzes epimerization, and StnR catalyzes a second round of transamination to complete the assembly of (2*S*,3*S*)-β-methyltryptophan.[22,23]

To confirm the role of *stnR* in streptonigrin biosynthesis, *stnR* was inactivated *in vivo* by replacing an internal fragment of *stnR* with the apramycin resistance cassette to generate WJN-1, and the genotype was verified by PCR (Supplementary Figure S1). To evaluate the effect of *stnR* replacement, the production of streptonigrin in WJN-1 was monitored by HPLC and LC-MS. Streptonigrin production was completely abolished in the strain WJN-1 and, surprisingly, two new compounds (**1** and **2**), absent in the wild-type strain, were present in the mutant strain WJN-1 (Figure 2 and Supplementary Figure S16).

Isolation and structural elucidation of 1 and 2 from *stnR* mutant WJN-1

The metabolic shift in the mutant WJN-1 prompted scale-up fermentation followed by multiple steps of silica gel and reverse C-18 column chromatography that afforded compounds **1** and **2** for structural elucidation. Compound **1** was obtained as a yellow crystal. The prolonged HPLC retention time compared with **2** under the same conditions and the UV-visible absorption profile were reminiscent of **2** (Figure 2). The high-resolution electrospray ionization MS analysis of **1** showed a quasimolecular $[M+H]^+$ ion peak at *m/z* 536.0713 (Supplementary Figure S8), corresponding to a quasimolecular formula of $C_{27}H_{18}ClNO_9$ (calcd 536.0743) with 19 degrees of

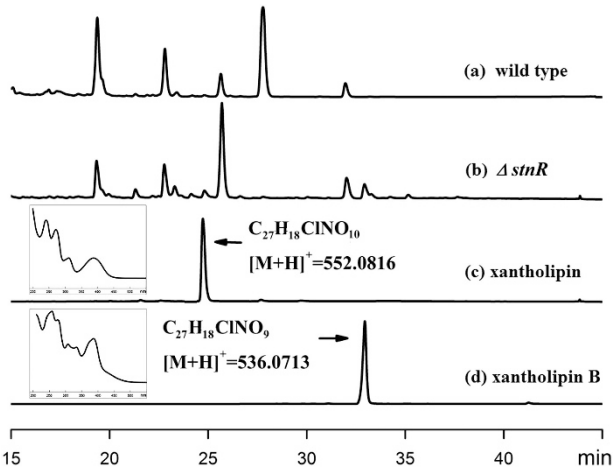

Figure 2 The production of xantholipin B (**1**) and xantholipin (**2**). HPLC profiles of the crude extracts from (**a**) *S. flocculus* CGMCC 4.1223 wild-type strain, (**b**) *stnR* mutant WJN-1, (**c**) xantholipin (**2**) and (**d**) xantholipin B (**1**). The arrows indicate compounds **1** and **2**. The inserted figures are the UV–vis spectra of **1** and **2**.

unsaturation that is 16 Da less than that of **2** ($C_{27}H_{18}ClNO_{10}$, *m/z*, 552.0816 $[M+H]^+$). The MS data indicated that **1** has one less oxygen atom than **2**. The IR spectrum indicated the presence of a hydroxyl group (3443 cm^{-1}) and carbonyl or amide groups (1642 and 1430 cm^{-1}) (Supplementary Figure S9).

The ^{13}C NMR and DEPT-135 spectra of **1** (Table 1) exhibited 27 carbon resonances that were attributed to 6 methyls or methines, 2 methylenes and 19 quaternary carbons. The ^{13}C NMR and heteronuclear single quantum coherence (HSQC) experiments on **1** also revealed a methyl (δ_C 19.7), a methylene (δ_C 30.2), a methoxy (δ_C 62.3), an oxymethine (δ_C 73.3), a dioxymethylene (δ_C 91.6) together with 20 aromatic/olefinic carbons (δ_C 95 ~ 155), an amide carbonyl (δ_C 167.8) and a carbonyl carbon (δ_C 182.3). In contrast, the ^{13}C NMR and HSQC spectra data for **2** indicated the presence of a methyl (δ_C 19.3), a methylene (δ_C 22.2), a methine (δ_C 53.8), a methoxy (δ_C 61.4), an oxymethine (δ_C 69.0), a quaternary carbon (δ_C 75.8), a dioxymethylene (δ_C 91.4) and a total of 16 aromatic/olefinic carbons (δ_C 95 ~ 155), an amide carbonyl group (δ_C 159.7) and 3 carbonyl carbons (δ_C 194.9, 192.4, 181.3).

The ^{13}C NMR spectra data of **1** and **2** revealed a close similarity. The main differences included that the carbonyl signals of a typical quinone at δ_C 194.9 and 192.4 disappeared in **1**, whereas a methine (δ_C 53.8) and a quaternary carbon (δ_C 75.8) adjacent to one oxygen atom in **2** were also absent in **1**. In the ^{13}C NMR spectrum of **1**, there were 4 more aromatic/olefinic carbons than in **2**, including 2 phenolic resonances at δ_C 151.4 and 152.7 and 2 quaternary carbons. Based on data in the literature, **2** was confirmed to be xantholipin,[9] and **1** is proposed to be its analog.

Because of limited skeletal protons in **1**, the connectivity of different carbons in **1** was established by interpretation of the heteronuclear multiple bond correlation (HMBC) data illustrated in Figure 3.

The ^1H NMR along with the HSQC spectra for **1** indicated the presence of four singlet signals of active protons at δ_H 13.34, 12.64, 11.75 and 8.69 in the low field, identified as three hydrogen-bonded OH protons and an amide proton. Based on the HMBC correlations of δ_H 12.64 coupled to C-18, C-19, C-20 and C-21, and δ_H 13.34 coupled to C-18, C-20 and C-22, these two hydroxyl groups are attached to C-19 and C-22, respectively. The proton resonances of H-17 at δ_H 3.68 (m, 1H) and the C-18 hydroxy proton at δ_H 6.41

Table 1 ^{1}H and ^{13}C NMR data for 1 and 2 (DMSO-*d*6)[a]

Position	1 [b]		2 [b]	
	δ_C (DEPT)	δ_H (mult, J/Hz)	δ_C (DEPT)	δ_H (mult, J/Hz)
1	133.9		133.4	
2	126.2	7.56 (d, 8.7)	125.5	7.52 (d, 8.6)
3	121.6	7.91 (d, 8.7)	120.5	7.78 (d, 8.6)
4	121.4		120.2	
5	145.4		150.0	
6	143.1		144.5	
8	139.4		142.9	
9	108.8		106.9	
10	182.3		181.3	
11	150.5		148.3	
12	113.3		116.3	
13	127.6		131.8	
14	131.1		132.5	
15	73.3	4.91 (dd, 6.1, 9.8)	69.0	5.34 (dd, 6.1, 9.8)
16	30.2	2.36 (dd, 9.8, 13.6), 3.61 (dd, 6.1, 13.6)	22.2	2.67 (m); 2.25 (m)
17	133.1		53.8	3.68 (m)
18	113.1		75.8	
19	152.7		192.4	
20	109.9		120.7	
21	130.7		144.6	
22	151.4		194.9	
23	101.1	6.67 (s)	98.5	6.11 (s)
24	138.7		152.8	
25-NH		11.75 (s)		12.20 (brs)
26	167.8		159.7	
27	19.7	2.25 (s)	19.3	2.18 (s)
28	91.6	5.43 (d, 5.8), 5.66 (d, 5.8)	91.4	5.50 (d, 6.1), 5.56 (d, 6.1)
29	62.3	4.07 (s)	61.4	4.01 (s)
11-OH		8.69 (s)		12.30 (s)
18-OH				6.41 (s)
19-OH		13.34 (s)		
22-OH		12.64 (s)		

[a]Peaks were assigned by analyses of the 1D and 2D NMR spectra.
[b]^{1}H NMR (600 MHz) and ^{13}C NMR (150 MHz).

(s, 1H) in **2** were absent in **1**, and the signals of C-17 and C-18 (δ_C 53.8 and 75.8) shifted downfield to δ_C 133.1 and 113.1. These observations suggested a hydroquinone group rather than a quinone group at the E ring of **1**. Likely because of the deshielding effect of the new aromatic ring of the E ring in **1**, the chemical shift of H-23 (δ_H 6.11, s) in **2** shifted downfield to δ_H 6.67.

The phenolic hydroxyl proton at C-11 (δ_H 8.69) on the C ring showed correlations to C-8, C-9, C-12 and C-13, suggesting the presence of a hydrogen bond with the carbonyl group, and hence ring C was connected to ring B at C-8 and C-9. A pair of *O*-coupling aromatic protons at δ_H 7.56 (1H, d, $J=8.7$ Hz) and 7.91 (1H, d, $J=8.7$ Hz) suggested the presence of a 1,2,3,4-tetrasubstituted benzene ring system, confirmed by the HMBC correlations of H-2 and H-3 to C-1, C-5 and C-6. A three-bond coupling of H-3 to C-10 indicated a carbonyl group to C-10 on the B ring, as shown in Figure 1. Therefore, a γ-pyrone system was assigned as **2**. The structure of **1** was similar to **2**, and a comparison of the xanthone moieties in the ^{13}C NMR spectra of both compounds indicated that a chloride atom is connected at C-1 (Table 1).

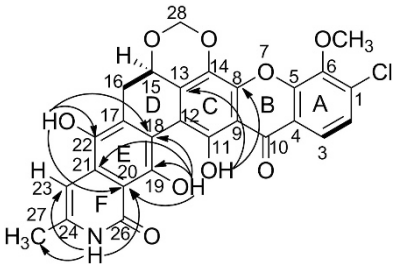

Figure 3 Select key ^{1}H-^{1}H COSY and HMBC correlations support the structural elucidation of xantholipin B (**1**). HMBC, heteronuclear multiple bond correlation.

Furthermore, the correlations of the proton at δ_H 11.75 to C-23 and C-27, the ^{13}C NMR chemical shift value of the remaining carbonyl group (δ_C 167.8) and the IR absorption at 1624 cm^{-1} indicated the presence of an amide moiety between C-20 and C-24. The conjunction of the lactam ring F with ring E in **1** was confirmed by the HMBC correlations of H-23 to C-20, C-21, C-24 and C-27, and H_3-27 to C-23 and C-24 (Figure 3).

Analysis of the ^{1}H-^{1}H COSY spectrum of **1** revealed the connectivity from H-15 to H_2-16, indicating the presence of a CH_2CHO group and a dioxolane group (O-CH_2-O) at δ_H 5.43, 5.66 (d, $J=5.8$ Hz) in **1**. Analysis of the HMBC correlations of the dioxolane H_2-28 to C-14 and C-15 and the oxymethine H-15 to C-12, C-13, C-16 and C-17 confirmed the attachment of the dioxolane at C-14 of the C ring and C-15 of the D ring in **1**.

On the basis of the ^{1}H-^{1}H COSY, HMQC and HMBC spectra of **1** (Figure 3), all protons were assigned unambiguously to their corresponding carbons. Thus, the planar structure of **1** was completely elucidated as shown in Figure 1. The ^{13}C and ^{1}H NMR spectral data of **1** and **2** are shown in Table 1. The absolute configuration of **2** was determined to be 15*R*, 17*S*, 18*R* by a modified Mosher's method,[9] and the $[\alpha]_D=-303.8°$ (*c* 0.53, dioxane). The ^{1}H-^{1}H coupling constants between H-15 and H-16 of **1** were consistent with those of **2** (Table 1), and the $[\alpha]_D$ of **1** was $-188.5°$ (*c* 0.53, dioxane), and hence the absolute configuration of **1** was also established to be 15*R*. Therefore, based on the full NMR analysis including 1D (^{1}H and ^{13}C) and 2D (^{1}H-^{1}H COSY, ^{1}H-^{13}C HSQC and ^{1}H-^{13}C HMBC) combined with comparisons with the published data, **1** was determined to be a new xantholipin congener for which the name xantholipin B is suggested (Figure 1).

Bioactivity evaluation of 1 and 2

Xanthone antibiotics are known for their cytotoxic and antibacterial activities. In this study, five human cancer cell lines, including KB, HL-60, BGC-803, A549 and MCF-7, were chosen to test the cytotoxicity of xantholipin B (**1**) and xantholipin (**2**) using the MTT (3-(4,5-dimethylthiazol-2-yl)-2,5-diphenyltetrazolium bromide) method.[24] The results in Table 2 indicate that both **1** and **2** exhibit potent activities and that **1** possesses even stronger cytotoxic effects than **2**. For example, the activity against the KB cell line is ~11-fold higher, and the activity against the BGC-803, A549 and MCF-7 cell lines is ~3–6-fold higher than that of **2**. Furthermore, **1** and **2** were tested for antibacterial activity against three Gram-positive bacteria, including *Bacillus mycoides*, *Staphylococcus aureus* and *Mycobacterium smegmatis*, and two Gram-negative bacteria, including *Escherichia coli* and *Klebsiella pneumoniae*, using a 96-well plate method.[25] As summarized in Table 3, both **1** and **2** demonstrate potent activity against Gram-positive bacteria, with MIC values ranging from 0.02 to

5 μg ml^{-1}, similar to the reported MIC values of **2** against other *S. aureus* and *B*acillus *subtilis* species.[9] Similar to the previous observation for the known xanthone antibiotics, these two compounds showed no activity against the Gram-negative bacteria *E. coli* and *K. pneumoniae*. Importantly, both **1** and **2** demonstrated noteworthy activity against methicillin-resistant *S. aureus* Mu50, with MIC values of 0.025 μg ml^{-1}. Both **1** and **2** were also tested for antifungal activity against *Candida albicans* and *Candida sake*. Compound **1** showed higher activity than **2** against both fungal species, with MIC values of 0.08–1.25 μg ml^{-1}. This is the first report to show the apparent antifungal activity of XAN family compounds (Table 3).

Xantholipin B supports the proposed xantholipin biosynthetic pathway

The cloning and sequencing of the XAN biosynthetic gene cluster from *S. flavogriseus* provided the opportunity to manipulate the XAN biosynthetic machinery by genetic engineering.[18] The XAN biosynthetic pathway features a type II polyketide synthase that is responsible for the assembly of the XAN skeleton and several oxidoreductases for catalyzing most of the post-polyketide synthase oxidative tailoring modification steps.[18] Analogous to the biosynthesis of XAN in *S. flavogriseus*, the same pathway could be proposed for *S. flocculus* CGMCC 4.1223 that harbors the same XAN gene cluster but which is silent under the culture conditions used for streptonigrin production. Interestingly, this silent gene cluster was activated when the aminotransferase-encoding gene *stnR*, which is unrelated to XAN biosynthesis, was replaced by the apramycin resistance cassette. However, the interrelationship between these two clusters remains to be elucidated. Importantly, the identification of xantholipin and xantholipin B from *S. flocculus* CGMCC 4.1223 WJN-1 provides evidence for the last steps of the previously proposed XAN biosynthetic pathway. The formation of the quinone ring E in **3** from **1** could be the result of adventitious oxidase activities (Figure 4a), and the subsequent reduction of the C17-C18 double bond may be catalyzed by reductase XanZ1/Z2 to give **4** (Figure 4b). In the last step, FAD-binding monooxygenase XanO5 can catalyze hydroxylation at C18 to generate the final product **2** from **4** (Figure 4c).

Table 2 The IC_{50} values of 1 and 2 against five tumor cell lines (μg ml^{-1})

	KB	*HL-60*	*BGC-803*	*A549*	*MCF-7*
1	0.036	0.0088	0.030	0.076	0.092
2	0.42	0.012	0.18	0.24	0.43

Table 3 The MIC values of 1 and 2 against microorganisms

	Tested microorganisms	*MIC/(μg ml^{-1})*	
		1	***2***
Gram-positive bacteria	*Bacillus mycoides*	0.08	0.08
	Mycobacterium smegmatis	5.0	5.0
	Staphylococcus aureus Mu50	0.025	0.025
Gram-negative bacteria	*Pseudomonas aeruginosa*	>30	>30
	Klebsiella pneumoniae	>30	>30
	Escherichia coli	>30	>30
Fungi	*Canidia albicans*	0.31	1.3
	Candida sake	0.080	0.31

METHODS

General experimental procedures

Optical rotation measurements were obtained on a JASCO P-1020 digital polarimeter (JASCO, Tokyo, Japan). IR spectra were measured on a Fourier Transform Infrared Spectrometer with KBr pellets (Thermo Fisher Scientific, Waltham, MA, USA). ^{1}H, ^{13}C, DEPT and 2D NMR spectra were recorded on a Bruker AM-600 spectrometer (Bruker, Karlsruhe, Germany) using DMSO-d_6 as the solvent and TMS as the internal reference. Chemical shifts (δ) were given in ppm, and coupling constants (J) were given in Hertz (Hz). Electrospray ionization-MS was performed on a LC-MS (Agilent Technologies, Santa Clara, CA, USA). Analytical and semi-preparative reversed-phase HPLC were performed on an Agilent series 1100 HPLC instrument equipped with a quaternary pump, a diode-array detector, an autosampler and a column compartment (Agilent Technologies). Materials for column chromatography contained silica gel (80–100 mesh and 200–300 mesh, Shanghai Shengya Chemical, Shanghai, China), reverse-phase silica gel (C18, 50 μm, YMC Company, Kyoto, Japan) and Sephadex LH-20 (40–70 mesh, General Electric Company, Fairfield, CT, USA). Other common chemical reagents were obtained from standard commercial sources and used directly.

DNA isolation and general manipulations

DNA isolation and manipulation in *E. coli* and *Streptomyces* were performed following standard procedures.[26,27] Primers were synthesized by Invitrogen (Shanghai, China). PCR amplifications were performed on a Veriti thermal cycler (Applied Biosystems, Carlsbad, CA, USA) using KOD-plus high-fidelity PCR polymerase (Toyobo, Osaka, Japan) or Taq DNA polymerase (Takara, Dalian, China).

Strains, plasmids and culture conditions

The strains and plasmids used in this study are listed in Supplementary Table S1. *S. flocculus* CGMCC 4.1223 was the producer of streptonigrin; *E. coli* DH10B and ET12567/pUZ8002 were used for subcloning and intergeneric conjugation, respectively; and *E. coli* BW25113/pIJ790 was used for gene replacement using a PCR targeting strategy.[28] *S. flocculus* CGMCC 4.1223 and its derivatives were cultivated at 30 °C in tryptic soy broth (TSB) liquid medium for growth of mycelia and on MS medium (2% mannitol, 2% soybean meal, 1.5% agar, pH 7.2) for sporulation and conjugation.

Construction of *stnR* mutant WJN-1

StnR was inactivated using a standard PCR targeting strategy based on λ_{Red} recombination.[28] Briefly, plasmid pLS1153 containing a partial streptonigrin

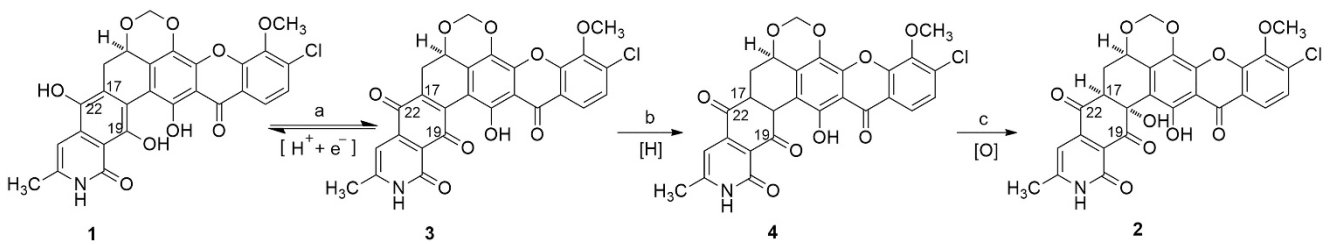

Figure 4 Proposed biosynthetic pathway of xantholipin B (**1**) to xantholipin (**2**).

gene cluster was used for *stnR* replacement to generate pLS1154 by using an apramycin resistance-*oriT* cassette that was amplified by the forward primer SftarstnR-For: 5′-CCCTACGGTGCCAGCCCCGCGGCGGTGGCCGCGGTGA CGATTCCGGGGATCCGTCGACC-3′ and the reverse primer SftarstnR-Rev: 5′-AATGCCGTGGTCGCGGGCCAGCACGTCCTGCGCCTCGGCTGTAGGC TGGAGCTGCTTC-3′. The mutated plasmid pLS1154 was introduced into *S. flocculus* CGMCC 4.1223 by intergeneric conjugation from *E. coli* ET12567/pUZ8002 to generate the Δ*stnR* double crossover mutant WJN-1 (Supplementary Figure S1A). The genetic phenotype of WJN-1 was further confirmed by PCR using the primers SftarstnA-T-For: 5′-ATCGAGGT GCACCTCGAC-3′ and SftarstnA-T-Rev: 5′-ACAGTTCCTTCGCGCCGAA-3′ (Supplementary Figure S1B).

Bacterial fermentation

The seed inoculum was prepared by inoculating 25 ml of seed medium (3.0% TSB, 0.5% yeast extract and 10.3% sucrose) with 50 μl of spore suspension in a 250 ml Erlenmeyer flask and incubating at 30 °C for 2 days on a rotary shaker (220 r.p.m.). Then, the seed cultures (25 ml) were transferred to 2 l Erlenmeyer flasks containing 500 ml of fermentation medium (2.5% glucose, 1.5% soybean flour, 0.5% NaCl, 0.5% KCl, 0.025% $MgSO_4{\cdot}7H_2O$, 0.3% K_2HPO_4, 0.3% $Na_2HPO_4{\cdot}12H_2O$, pH 7.2) along with 10% sterilized Amberlite XAD-16 (Mitsubishi, Tokyo, Japan) and were incubated at 30 °C for 6 additional days.

Extraction, isolation, HPLC analysis and structural elucidation

The 50 l of fermentation broth was centrifuged (5000 r.p.m., 10 min) to separate the mycelia and Amberlite XAD-16 resin. The resin was extracted three times with 50 l of EtOAc, and the mycelia were extracted three times with 10 l of EtOAc. The combined organic extracts were concentrated under reduced pressure, and the resulting crude extract (8 g) was applied to a normal-phase silica gel column (200–300 mesh, 90 g) with a gradient elution system of $CHCl_3/CH_3OH$ (100/0, 100/1, 50/1, 25/1, 10/1, 1/1 and 0/100, v/v, 400 ml each) to yield six fractions (Fr.1–Fr.6) based on HPLC analysis. Fr.1 and Fr.2 were combined, concentrated under vacuum and loaded onto a chromatography column packed with reverse-phase silica gel. The column was eluted by a linear gradient of methanol/water (40–100%) to yield five subfractions (Fr.1.1–Fr.1.5). The eluate was monitored by HPLC at 254 nm. Fr.1.2 (16 mg) was evaporated to dryness and further purified on a Sephadex LH-20 chromatography column to yield **1** (8 mg). Residues from Fr.1.3 (12 mg) were further purified on a Sephadex LH-20 column to yield **2** (5 mg). The structures of the purified compounds were elucidated by a combination of 1D (^1H and ^{13}C) and 2D (^1H-^1H COSY, HSQC, and HMBC) NMR analysis (Supplementary Figures S2–S7 and S10–S15), HR-ESI-MS analysis (Supplementary Figure S8) and by comparison of the spectra with published data. The NMR data are summarized in Table 1, and the IR spectrum of **1** is shown in Supplementary Figure S9.

Cytotoxicity assay

The two compounds were evaluated for cytotoxic effects by MTT assay on the following cell lines: KB (human oral epithelial carcinoma cell line), HL-60 (myelogenous leukemia cells), BGC-803 (human gastric cells, poorly differentiated), A549 (non-small-cell lung carcinoma cells) and MCF-7 (human breast carcinoma cells). The MTT assay was based on the protocol described by Mosmann[24] with minor modifications. Briefly, the cell lines were grown in cell culture media at 37 °C under a humidified atmosphere of 5% CO_2. Subsequently, 10 μl serially diluted solutions of compounds (100, 10, 1, 0.1, 0.01 or 0.001 μg ml^{-1}) were added to 90 μl aliquots of cell suspension (10^5 cells ml^{-1}) in 96-well plates after incubation for 6 h and were further incubated for 48 h. The MTT solution (10 μl, 5 mg ml^{-1}) was then pipetted into each well and incubated for 4 h. The medium containing MTT was removed and DMSO (100 μl) was added to dissolve any formed formazan crystals. The IC_{50} values were obtained by software analysis.

Antimicrobial assay

The antimicrobial assay was performed using the 96-well micro-plate-based broth dilution method.[25] The compounds were dissolved in DMSO to 10 mg ml^{-1} as a stock solution. All samples were diluted in culture media to 5 μg ml^{-1} as the initial concentration. Further 1:2 serial dilutions were performed by the addition of broth to reach concentrations ranging from 2.5 to 0.0048 μg ml^{-1}. A 100 μl aliquot of each dilution was distributed into 96-well plates as well as blank controls (without inoculation or compounds) and growth controls (containing culture medium plus DMSO, without compounds). Five species of bacteria, *E. coli*, *K. pneumoniae*, *B. mycoides*, *S. aureus* Mu50 and *M. smegmatis*, were used for the assay. Each well, excluding the blank control, was inoculated with 5 μl of bacterial suspension (~10^5 CFUs per well) and incubated at 37 °C for 16 h. Antifungal testing against *C. albicans* and *C. sake* followed the same procedure but with incubation at 30 °C and using concentrations ranging from 30 to 0.04 μg ml^{-1}. After incubation, microbial growth was measured by monitoring optical density at 600 nm on a Synergy 2 multi-mode microplate reader (BioTek, Winooski, VT, USA), and the lowest concentration in the dilution series that did not demonstrate growth was designated the MIC of the compounds.

CONCLUSIONS

XAN is a polycyclic xanthone antibiotic with unique structural features and extensive bioactivity that has recently been identified as a candidate compound for fibrotic disease treatment.[17] In this work, we report an alternative XAN producer, *S. flocculus* CGMCC 4.1223 WJN-1, and isolated a new XAN analog, xantholipin B. Our results indicate that both compounds possess potent cytotoxicity against a wide range of human cancer cell lines, whereas xantholipin B exhibits greater cytotoxicity than XAN. Furthermore, this is the first report to show the antifungal activity of XANs. The identification of xantholipin B provides new insights into the structure–activity relationship of XANs as antitumor compounds, broadens the understanding of the XAN biosynthetic pathway and sets the stage for the generation of xantholipin analogs with enhanced activity by bioengineering of the XAN biosynthetic pathway.

CONFLICT OF INTEREST

The authors declare no conflict of interest.

ACKNOWLEDGEMENTS

We thank Professor Lefu Lan at Shanghai Institute of Materia Medica CAS for technical support for the antibacterial assay and Professor Longhai Shen at China State Institute of Pharmaceutical Industries for performing the antitumor activity assay. We also thank the Instrumental Analysis Center of Shanghai Jiao Tong University and Shanghai Organic Chemistry for providing spectroscopic analyses. We are grateful to Dr Mostafa E Rateb for critical reading of the manuscript. This work was supported by grants from the National Natural Science Foundation of China (31425001 to SL; 31121064 to ZD) and grants from MOE of China.

1 Newman, D. & Cragg, G. Natural products as sources of new drugs over the 30 years from 1981-2010. *J. Nat. Prod.* **75**, 311–335 (2012).
2 Luo, Y. *et al.* Engineered biosynthesis of natural products in heterologous hosts. *Chem. Soc. Rev.* **44**, 5265–5290 (2015).
3 Luo, Y. *et al.* Activation and characterization of a cryptic polycyclic tetramate macrolactam biosynthetic gene cluster. *Nat. Commun.* **4**, 2894–2899 (2013).
4 Scherlach, K. & Hertweck, C. Triggering cryptic natural product biosynthesis in microorganisms. *Org. Biomol. Chem.* **7**, 1753–1760 (2009).
5 Aigle, B. & Corre, C. Waking up *Streptomyces* secondary metabolism by constitutive expression of activators or genetic disruption of repressors. *Methods Enzymol.* **517**, 343–366 (2012).
6 Medema, M., Breitling, R., Bovenberg, R. & Takano, E. Exploiting plug-and-play synthetic biology for drug discovery and production in microorganisms. *Nat. Rev. Microbiol.* **9**, 131–137 (2011).
7 Nett, M., Ikeda, H. & Moore, B. S. Genomic basis for natural product biosynthetic diversity in the actinomycetes. *Nat. Prod. Rep.* **26**, 1362–1384 (2009).
8 Zerikly, M. & Challis, G. L. Strategies for the discovery of new natural products by genome mining. *ChemBioChem* **10**, 625–633 (2009).
9 Terui, Y. *et al.* Xantholipin, a novel inhibitor of HSP47 gene expression produced by *Streptomyces* sp. *Tetrahedron Lett.* **44**, 5427–5430 (2003).

10 Drautz, H., Keller-Schierlein, W. & Zahner, H. Metabolic products of microorganisms, 149. Lysolipin I, a new antibiotic from streptomyces violaceoniger (author's transl). *Arch. Microbiol.* **106**, 175–190 (1975).
11 Fukushima, K., Ishiwata, K., Kuroda, S. & Arai, T. Identity of antibiotic P-42-1 elaborated by *Actinomyces tumemacerans* with kanchanomycin and albofungin. *J. Antibiot. (Tokyo)* **26**, 65–69 (1973).
12 Kobayashi, K. *et al.* Actinoplanones C, D, E, F and G, new cytotoxic polycyclic xanthones from *Actinoplanes* sp. *J. Antibiot. (Tokyo)* **41**, 741–750 (1988).
13 Kobayashi, K. *et al.* Actinoplanones A and B, new cytotoxic polycyclic xanthones from *Actinoplanes* sp. *J. Antibiot. (Tokyo)* **41**, 502–511 (1988).
14 Nakagawa, A., Iwai, Y., Shimizu, H. & Omura, S. Enhanced antimicrobial activity of acetyl derivatives of cervinomycin. *J. Antibiot. (Tokyo)* **39**, 1636–1638 (1986).
15 Nakagawa, A., Omura, S., Kushida, K., Shimizu, H. & Lukacs, G. Structure of cervinomycin, a novel xantone antibiotic active against anaerobe and mycoplasma. *J. Antibiot. (Tokyo)* **40**, 301–308 (1987).
16 Tanaka, H., Kawakita, K., Suzuki, H., Spiri-Nakagawa, P. & Omura, S. The mode of action of cervinomycin in *Staphylococcus aureus*. *J. Antibiot. (Tokyo)* **42**, 431–439 (1989).
17 Winter, D. K., Sloman, D. L. & Porco, J. A. Polycyclic xanthone natural products: structure, biological activity and chemical synthesis. *Nat. Prod. Rep.* **30**, 382–391 (2013).
18 Zhang, W. *et al.* Unveiling the post-PKS Redox tailoring steps in biosynthesis of the Type II polyketide antitumor antibiotic xantholipin. *Chem. Biol.* **19**, 422–432 (2012).
19 Xu, F. *et al.* Characterization of streptonigrin biosynthesis reveals a cryptic carboxyl methylation and an unusual oxidative cleavage of a N-C bond. *J. Am. Chem. Soc.* **135**, 1739–1748 (2013).
20 Hartley, D. L. & Speedie, M. K. A tryptophan *C*-methyltransferase involved in streptonigrin biosynthesis in *Streptomyces flocculus*. *Biochem. J.* **220**, 309–313 (1984).
21 Gould, S. & Chang, C. C. Studies of nitrogen metabolism using ^{13}C NMR spectroscopy. 1. Streptonigrin biosynthesis. *J. Am. Chem. Soc.* **100**, 1624–1626 (1978).
22 Zou, Y. *et al.* Stereospecific biosynthesis of β-methyltryptophan from L-tryptophan features a stereochemical switch. *Angew. Chem. Int. Ed.* **52**, 12951–12955 (2013).
23 Kong, D. *et al.* Identification of (2*S*,3*S*)-β-methyltryptophan as the real biosynthetic intermediate of antitumor agent streptonigrin. *Sci. Rep.* **6**, 20273–20281 (2016).
24 Mosmann, T. Rapid colorimetric assay for cellular growth and survival: application to proliferation and cytotoxicity assays. *J. Immunol. Methods* **65**, 55–63 (1983).
25 Kumarasamy, Y., Cox, P., Jaspars, M., Nahar, L. & Sarker, S. Screening seeds of Scottish plants for antibacterial activity. *J. Ethnopharmacol.* **83**, 73–77 (2002).
26 Sambrook, J., Fritsch, E. F. & Maniatis, T. *Molecular Cloning: A Laboratory Manual* Second EditionCold Spring Harbor Laboratory Press, Cold Spring Harbor, NY, (1989).
27 Kieser, T., Bibb, M., Chater, K. F., Butter, M. & Hopwood, D. *Practical Streptomyces Genetics: A Laboratory Manual* (John Innes Foundation, Norwich, UK, 2000).
28 Gust, B., Challis, G., Fowler, K., Kieser, T. & Chater, K. PCR-targeted *Streptomyces* gene replacement identifies a protein domain needed for biosynthesis of the sesquiterpene soil odor geosmin. *Proc. Natl Acad. Sci. USA* **100**, 1541–1546 (2003).